FULL PAPER

An improved apparent polar wander path for southwest Japan: post-Cretaceous multiphase rotations with respect to the Asian continent

Koji Uno[1*] , Yuta Idehara[1], Daichi Morita[1] and Kuniyuki Furukawa[2]

Abstract

To construct the Mesozoic apparent polar wander path (APWP) for the inner arc of the southwestern Japanese islands (referred to as southwest Japan) and compare it to that of East Asia, a 110 Ma paleomagnetic pole for southwest Japan was determined. Mudstone and sandstone samples were collected from 16 sites for paleomagnetic analysis in the Lower Cretaceous Inakura Formation of the Inakura area in the central part of southwest Japan. A high-temperature magnetization component, with unblocking temperatures of 670–695 °C, was isolated from 12 sites of red mudstone. Of these, 11 sites revealed a primary remanent magnetization during the Early Cretaceous. The primary directions combined with the previously reported ones provide a new mean direction ($D = 79.7°$, $I = 47.4°$, $a_{95} = 6.5°$, $N = 17$), and a corresponding paleomagnetic pole that is representative of southwest Japan (24.6° N, 203.1° E, $A_{95} = 6.8°$). The Early Cretaceous paleomagnetic pole, together with the Late Cretaceous and Cenozoic poles, constitute a new APWP for southwest Japan. The new APWP illustrates a standstill polar position during 110–70 Ma, suggesting tectonic quiescence of this region. This standstill was followed by two large tracks during the Cenozoic. We interpret these tracks as clockwise tectonic rotations of southwest Japan that occurred twice during the Cenozoic. The earlier tectonic rotation occurred for a tectonic unit positioned below northeast China, the Liaodong and Korean Peninsulas, and southwest Japan (East Tan-Lu Block) during the Paleogene. The later rotation took place only under southwest Japan during the Neogene. Cenozoic multiphase rifting activity in the eastern margin of the Asian continent was responsible for the tectonic rotations that are observed from the paleomagnetic studies. Intermittent rifting may constitute a series of phenomena due to asthenospheric convection, induced by the growth of the Eurasian mega-continent in the Mesozoic.

Keywords: Apparent polar wander path, Cretaceous, Southwest Japan, East Asia

Introduction

Apparent polar wander paths (APWPs) for cratonic blocks are useful in understanding the paleogeographic evolution of a region over geological time scales. The APWPs for the eastern Asia blocks, constructed from the Paleozoic to the present, provide the age of amalgamation and associated closure of the ocean between these blocks (e.g., Enkin et al. 1992; Wu et al. 2017; Huang et al. 2018a). For example, the North and South China Blocks shared positions of coeval paleomagnetic poles from the Middle to Late Jurassic (Gilder and Courtillot 1997; Yang and Besse 2001), indicating complete amalgamation between these blocks to form the composite Chinese Block (Xu et al. 1997). Additionally, the poles for the composite Chinese Block coincide with those for the

*Correspondence: unokoji@okayama-u.ac.jp
[1] Department of Earth Sciences, Okayama University, 3-1-1 Tsushimanaka, Kita-ku, Okayama 700-8530, Japan
Full list of author information is available at the end of the article

Uno *et al. Earth, Planets and Space*   (2021) 73:132

Page 2 of 17

Siberia Block since the Early Cretaceous (Van der Voo et al. 2015; Ren et al. 2016), and is interpreted as the final closure of the Mongol-Okhotsk Ocean.

APWPs are fundamental earth science data, even for smaller geological domains, such as island arcs. The inner arc of the southwestern Japanese islands (henceforth referred to as southwest Japan) is an island arc system having a specific kinematic history (e.g., Maruyama et al. 1997; Taira 2001; Isozaki et al. 2010; Isozaki 2019). The Cenozoic segment of the APWP for southwest Japan suggests the opening of the Japan Sea in the Miocene (Otofuji and Matsuda 1987; Kodama and Takeda 2002). The pre-Miocene poles for this region are shifted toward lower latitudes with respect to the coeval poles for the eastern Asia blocks (Otofuji 1996), indicating that southwest Japan drifted from the continent due to the opening of the Japan Sea during the Miocene. Southwest Japan drifted in a clockwise rotation of ~40° about a pivot located at the western end of this region (Ishikawa 1997; Uno 2002; Hoshi 2018).

At present, the APWP for southwest Japan is not significantly older than the Late Cretaceous (Uno et al. 2017). Little effort has been made to construct the Mesozoic APWP for southwest Japan, as more importance has been given to the Cenozoic event, i.e., the Miocene opening of the Japan Sea. Mesozoic southwest Japan

constitutes an integral part of the continental margin of East Asia (Otofuji et al. 1985; Jolivet et al. 1994; Nohda 2009; Ishida et al. 2003; Lee 2008). Southwest Japan can be an important data source for the analysis of the Mesozoic tectonics of East Asia, particularly to understand the spatial extent of tectonic activity in the continent. The construction of the Mesozoic APWP for southwest Japan would contribute to elucidating the intracontinental deformation history along the eastern margin of East Asia since the Mesozoic.

The Mesozoic southwest Japan pole that first needs to be established is an Early Cretaceous pole at 110 Ma since the previously reported 110 Ma pole positions for this region (Sasayama area; Sy in Fig. 1a) are not consistent (Fig. 1b; Shibuya and Sasajima 1984; Uno and Furukawa 2005; Tsuji and Morinaga 2008). In contrast, the coeval poles for East Asia agree well with each other (Cogné et al. 2013; Ren et al. 2016; Wu et al. 2017). Thus, ambiguity remains in the Cretaceous segment of the APWP for southwest Japan. The use of the 110 Ma poles for southwest Japan gives polar distances ranging from 45° to 75° relative to East Asia, suggesting uncertainty in relative motion (Fig. 1b). The determination of the 110 Ma pole for southwest Japan allows further extension of the APWP segment toward older ages and offers an understanding of the relative motion that occurred
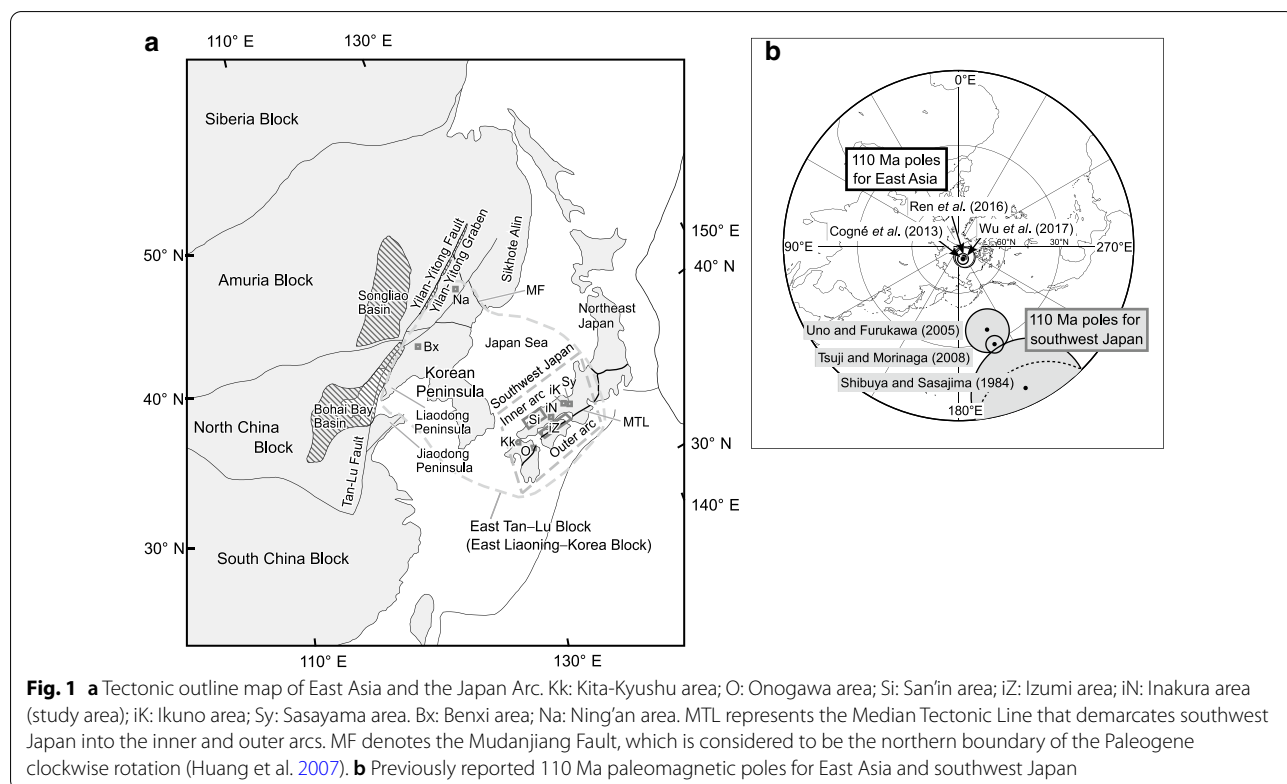
Fig. 1 a Tectonic outline map of East Asia and the Japan Arc. Kk: Kita-Kyushu area; O: Onogawa area; Si: San'in area; iZ: Izumi area; iN: Inakura area (study area); iK: Ikuno; Sy: Sasayama area. Bx: Benxi area; Na: Ning'an area. MTL represents the Median Tectonic Line that demarcates southwest Japan into the inner and outer arcs. MF denotes the Mudanjiang Fault, which is considered to be the northern boundary of the Paleogene clockwise rotation (Huang et al. 2007). **b** Previously reported 110 Ma paleomagnetic poles for East Asia and southwest Japan

Uno *et al. Earth, Planets and Space* (2021) 73:132

Page 3 of 17

in the eastern margin of the Asian continent since the Cretaceous.

The Lower Cretaceous (110 Ma) Inakura Formation in the Inakura area (34.55° N, 133.46° E), the central part of southwest Japan (iN; Fig. 1a), was selected as the study site. This area is the most suitable for providing reliable paleomagnetic data for southwest Japan, as the land on which the Inakura Formation was deposited is considered to be the most well-preserved continental tectonic unit of southwest Japan (Matsubara et al. 2017; Sonehara et al. 2020). We present new paleomagnetic data from the Inakura area and provide an Early Cretaceous paleomagnetic pole, representative of southwest Japan. This pole has been incorporated into the paleomagnetic database for southwest Japan and defines the APWP for this region from the Early Cretaceous onward.

Geological setting and sampling

In East Asia, non-marine Lower Cretaceous sedimentary rocks are widely distributed in the North and South China Blocks, Indochina Block, northeast China, and Far East Russia (Racey 2009; Yan et al. 2019). Such rocks are also extensively found in the southwestern part of the Korean Peninsula, and are named the Gyeongsang Supergroup (Kang and Paik 2013). The coeval sedimentary rocks in southwestern Japan are scattered across the Kitakyushu (Kanmon Group), Inakura (Inakura Formation), and Sasayama (Sasayama Group) areas from west to east (Kk, iN, and Sy, respectively; Fig. 1a) (Tachibana and Suzuki 2010).

The Inakura Formation, in the Inakura area, unconformably overlies the Permian Maizuru Group, and is overlain by Paleogene sedimentary rocks (Imamura and Kusumi 1951; Matsuura et al. 2002; Tachibana and Suzuki 2010) (Fig. 2). This formation is divided into three members: the Nishinotani conglomerate, Yamaji mudstone, and Ishizuchiyama reddish mudstone, in ascending order (Tachibana and Suzuki 2010). The Nishinotani conglomerate and Yamaji mudstone members are composed of alluvial fan and lacustrine deposits, respectively, whereas the Ishizuchiyama reddish mudstone member consists of floodplain deposits with red-colored clasts. The upper part of the Inakura Formation, including the Ishizuchiyama reddish mudstone member, is paleontologically correlated with the Shimonoseki Subgroup, that is, the upper part of the Kanmon Group, in the Kitakyushu area (Kobayashi 1990). The Shimonoseki Subgroup provided hornblende K–Ar ages of 105.2 ± 3.3 and 106.7 ± 3.3 Ma (Imaoka et al. 1993), zircon U–Pb age of 106.3 ± 0.7 Ma (Miyazaki et al. 2016), and fission-track ages of 115.4 ± 3.8 and 117 Ma (Murakami 1985; Kimura 1996). The Inakura
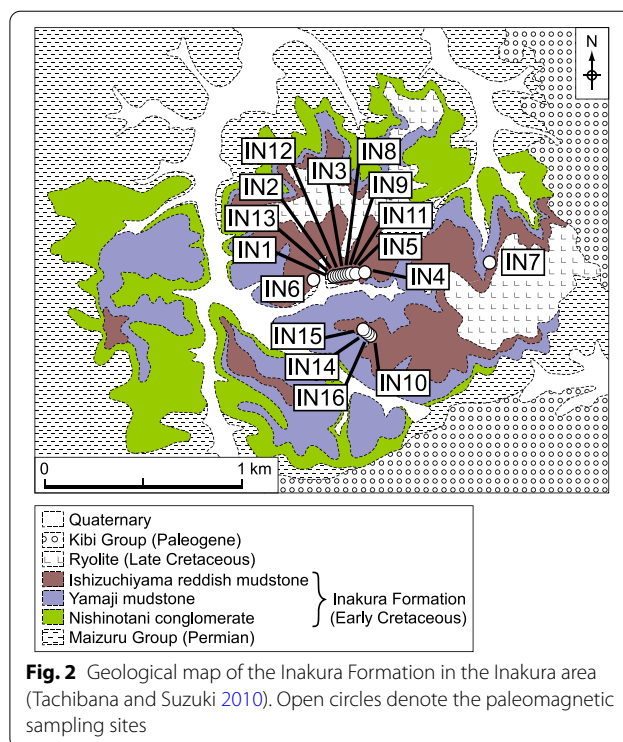
Fig. 2 Geological map of the Inakura Formation in the Inakura area (Tachibana and Suzuki 2010). Open circles denote the paleomagnetic sampling sites

Formation lacks radiometric dates, but its upper part is assigned to the Early Cretaceous (~110 Ma) based on the age of the equivalent Kanmon Group. The geological structure of the Inakura Formation is described as a basin with gentle dips < 20° (Imamura and Kusumi 1951). The age of tilting was directly constrained to be earlier than 55.2 Ma, when the overlying horizontal Paleogene sediments (55.2 ± 3.3 Ma fission-track ages, Matsuura et al. 2002) covered the Inakura Formation. In addition, the neighboring mid-Cretaceous (~100 Ma) formation revealed horizontal attitudes (Suzuki et al. 2001), suggesting that the tilting of the Inakura Formation most likely occurred prior to 100 Ma.

Samples of red mudstone (sites IN1–IN6, IN8–IN10, and IN13–IN16), greenish red mudstone (sites IN11 and IN12), and gray fine sandstone (site IN7) from the Ishizuchiyama reddish mudstone member were collected at 16 sites for paleomagnetic analysis (Fig. 2). Six to nine samples were collected from each site. The strata in the sampling sites were horizontal to gently dipping (< 20°), but the strata in site IN6 were steeply dipping. All samples were manually collected and were oriented in the field with a magnetic compass attached to a tripod. The present-day geomagnetic field declinations at the sampling sites were determined using the International Geomagnetic Reference Field (IGRF) model (Thébault et al. 2015).

Uno *et al. Earth, Planets and Space*   (2021) 73:132

Page 4 of 17

Methods

Paleomagnetism

In the laboratory, the oriented hand samples were cored and cut into cylindrical specimens, each with a diameter of 25 mm and a length of 22 mm. Natural remanent magnetizations (NRMs) were measured using a Natsuhara SMM-85 spinner magnetometer at Okayama University. All samples were subjected to progressive thermal demagnetization, using a Natsuhara TDS-1 thermal demagnetizer, in a series of 100 °C steps to 200 °C, 50 °C steps between 200 and 500 °C, and 40 °C steps between 500 and 620 °C. Demagnetization steps of 5 °C or 10 °C were used at temperatures above 650 °C. The results for each sample were plotted on orthogonal vector diagrams (Zijderveld 1967) to evaluate the demagnetization behavior (Fig. 3). Principal component analysis (Kirschvink 1980) was used to estimate the directions of the observed magnetic components. The maximum angular deviations (MADs) of the least square fits never exceeded 20° and rarely exceeded 15°. Paleomagnetic data were analyzed using the software applications of Cogné (2003) and Hatakeyama (2018).

Rock magnetism

Rock magnetic experiments were conducted on the selected red mudstone samples. Progressive thermal demagnetization of a three-component isothermal remanent magnetization (IRM; Lowrie 1990), in fields of 2.5 T (high-coercivity component), 0.4 T (medium-coercivity component), and 0.12 T (low-coercivity component), was conducted using a Magnetic Measurements MMPM10 pulse magnetizer to identify the ferromagnetic mineral content.

We measured the anisotropy of magnetic susceptibility (AMS) of the red mudstone samples using an AGICO KLY-3 susceptibility bridge. This was used to evaluate the bulk magnetic fabric, which is affected by paramagnetic and diamagnetic minerals that are not carriers of NRM as well as ferromagnetic minerals. AMS can be represented by an ellipsoid with three principal axes, denoted as $k_{max} \geq k_{int} \geq k_{min}$. The shape parameter T and the degree of anisotropy P' were calculated using Jelínek's (1981) method.

To obtain a high-fidelity record of the Early Cretaceous magnetic field of the Inakura area, we assessed the inclination shallowing of the remanent magnetization component of the Inakura Formation using the anisotropy of the IRM and the correction method of Hodych and Buchan (1994). A representative sample was selected from each site. A magnetic field of up to 800 mT was progressively applied at 45° to the bedding plane of the samples to avoid field-impressed anisotropy. The IRM was measured at each step parallel (IRM_X), and perpendicular (IRM_Z) to the bedding plane. The IRM_Z was plotted against IRM_X, and the IRM_Z/IRM_X ratio was calculated based on the slope of the least-square-fit line for each plot. This ratio can be used to determine the amount of inclination shallowing using $\tan I_N / \tan I_F = IRM_Z/IRM_X$, where I_N is the inclination of remanence and I_F the inclination of the field in which it was acquired.

Optical observations

The polished thin sections of red mudstone samples were examined under a Carl Zeiss optical microscope at the Okayama University to identify the occurrence and textural position of iron oxides.
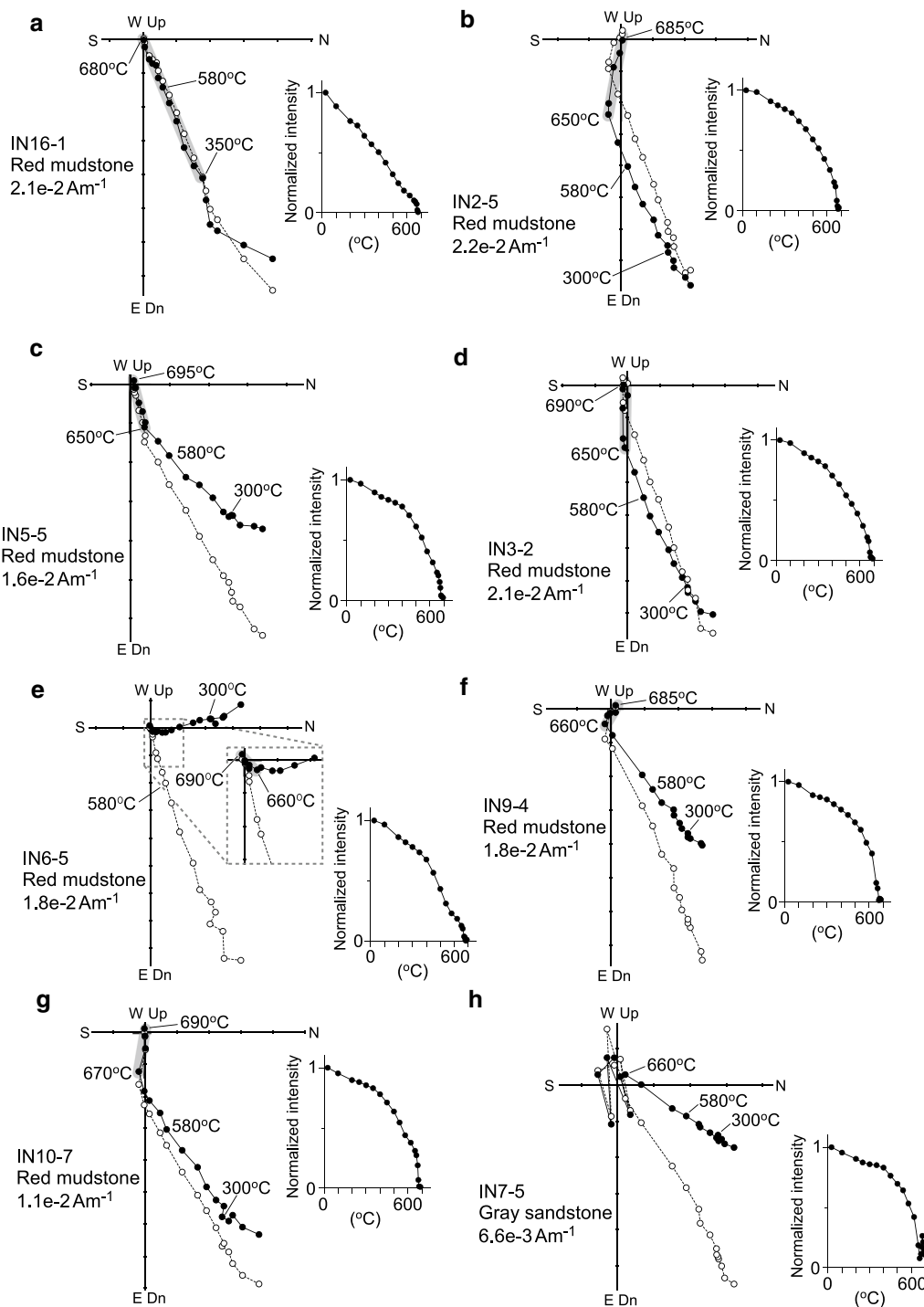
Results

Paleomagnetism

Initial NRM intensities ranged between 6.1×10^{-2} and 5.8×10^{-3} Am^{-1}. Samples of red and greenish red mudstone had higher intensities (averaging 1.7×10^{-2} Am^{-1}), whereas those of gray sandstone had lower intensities (averaging 7.3×10^{-3} Am^{-1}).

Thermal demagnetization revealed a stable high-temperature component from 12 sites that decays to the origin on the orthogonal plots (Table 1, Fig. 3). This component was identified after removal of a medium-temperature component at 250–300 °C for two sites (IN15 and IN16; Fig. 3a) and at 620–670 °C for 10 sites (IN1–IN3, IN5, IN6, IN8–IN10, IN13, and IN14; Fig. 3b–g), and in 80% of the cases, the unblocking temperatures of the medium-temperature component ranged from 650 to 660 °C. The unblocking temperatures of the high-temperature component ranged from 670 to 695 °C (Fig. 3a–g), suggesting hematite to be the predominant carrier of the remanent magnetization. The high-temperature component was derived exclusively from the red mudstone samples (at the 12 sites). The remaining four sites (IN4, IN7, IN11, and IN12) did not show significant higher-temperature trajectories (Fig. 3h).

The high-temperature components of the 12 sites showed a normal polarity. The precision parameter (k value) of the 12 site-mean directions ranged from 13.3 to 553.8 (Table 1). Before tilt correction, the mean field direction was $D = 81.8°$ and $I = 46.3°$ with $\alpha_{95} = 12.2°$ ($N = 12$). These values are significantly different from the Earth's present field direction ($D = 352.4°$, $I = 49.2°$) as well as the predicted direction, based on the geocentric axial dipole field ($D = 0.0°$, $I = 54.0°$), in the study area (Fig. 4a). The mean direction after tilt correction was $D = 86.5°$ and $I = 36.1°$, with $\alpha_{95} = 9.3°$ ($N = 12$). Notably, site IN6 is an outlier in the dataset. This site had a steep dip of 107° (Table 1), and its tilt-corrected direction was horizontal (Fig. 4a). The mean directions were

Fig. 3 Representative orthogonal plots in geographic coordinates and normalized remanence intensity curves of the thermal demagnetization results. Solid and open symbols on orthogonal plots represent projections on the horizontal and vertical planes, respectively. The highlighted magnetization component denotes the high-temperature remanent magnetization

calculated based on the remaining 11 sites, before and after tilt correction as $D = 83.0°$, $I = 41.9°$ with $\alpha_{95} = 7.9°$ and $D = 84.3°$, $I = 39.1°$ with $\alpha_{95} = 6.9°$, respectively. Tilt

correction increased the precision parameter from 34.2 to 44.4, and the fold test of McFadden (1990) was positive at the 95% confidence level with in situ $\xi_2 = 6.61$,

Table 1 Site and formation mean paleomagnetic results from southwest Japan at 110 Ma

Site	Formation	Lithology	N(n)	In situ D (°)	In situ I (°)	Tilt corrected D (°)	Tilt corrected I (°)	I corrected D (°)	I corrected I (°)	k	α_{95} (°)	Locality Lat (°N)	Long (°E)	Strike (°)	Dip (°)	IRM_Z/IRM_X
High-temperature component																
IN1	Inakura	Red ms	4(6)	94.2	27.9	94.2	27.9	94.2	29.2	70.3	11.0	34.55	133.46	0	0	0.940
IN2	Inakura	Red ms	6(6)	91.8	31.6	91.8	31.6	91.8	33.7	25.3	13.6	34.55	133.46	0	0	0.907
IN3	Inakura	Red ms	7(7)	77.0	25.3	77.0	25.3	77.0	26.6	13.6	17.0	34.55	133.46	0	0	0.938
IN4	Inakura	Red ms	(6)									34.55	133.46	97	17	
IN5	Inakura	Red ms	6(6)	69.3	51.6	70.0	42.6	70.0	43.0	34.9	11.5	34.55	133.46	344	9	0.977
IN6[a]	Inakura	Red ms	6(6)	296.1	72.8	105.0	0.0	105.0	0	23.6	14.1	34.55	133.46	18	107	
IN7	Inakura	Gray fine ss	(7)									34.55	133.47	89	11	
IN8	Inakura	Red ms	6(6)	71.3	37.5	70.1	40.0	70.1	42.9	40.6	10.6	34.55	133.46	192	3	0.859
IN9	Inakura	Red ms	9(9)	89.0	49.9	88.2	52.8	88.2	57.8	13.3	14.7	34.55	133.46	192	3	0.830
IN10	Inakura	Red ms	8(8)	88.8	46.2	85.5	36.9	85.5	39.6	58.3	7.3	34.55	133.46	335	10	0.906
IN11	Inakura	Greenish Red ms	(6)									34.55	133.46	292	3	
IN12	Inakura	Greenish Red ms	(6)									34.55	133.46	0	0	
IN13	Inakura	Red ms	5(6)	95.4	30.8	95.4	30.8	95.4	35.3	27.7	14.8	34.55	133.46	0	0	0.840
IN14	Inakura	Red ms	6(6)	87.2	56.7	95.2	49.9	95.2	54.4	277.8	4.0	34.55	133.46	42	9	0.850
IN15	Inakura	Red ms	6(6)	77.7	55.7	86.8	49.9	86.8	51.4	433.0	3.2	34.55	133.46	42	9	0.950
IN16	Inakura	Red ms	4(6)	66.6	42.2	73.4	38.0	73.4	42.3	553.8	3.9	34.55	133.46	42	9	0.858
In situ mean			11	83.0	41.9					34.2	7.9		133.46			
Tilt-corrected mean						84.3	39.1			44.4	6.9					
Inclination-corrected mean								84.2	41.9	42.0	7.1					
Uno and Furukawa (2005)																
SG1[b]	Ohyamashimo	Red ms	6(6)	39.7	44.8	58.1	48.1			24.9	15.6					
SG2[b]	Ohyamashimo	Red ss	5(5)	140.8	82.2	51.4	68.3			366.8	4.0					
SG3[b]	Ohyamashimo	Red ms	6(6)	45.8	42.6	63.1	48.2			49.0	9.7					
SG8[b]	Ohyamashimo	Red ms	6(6)	64.8	53.9	91.2	60.6			95.3	6.9					
SG12[b]	Ohyamashimo	Red ms	7(7)	51.8	40.1	71.7	57.1			119.9	5.5					
SG13[b]	Ohyamashimo	Red ms	3(6)	52.8	40.3	74.0	56.0			88.3	13.2					
In situ overall mean			17	73.8	46.1					18.0	8.6	34.55	133.46			
Tilt-corrected overall mean						79.8	45.6			28.6	6.8					
Inclination-corrected overall mean								79.7	47.4	31.0	6.5					
Medium temperature component																
In situ mean			12	58.2	50.6					81.7	4.8	34.55	133.46			
Tilt-corrected mean						59.9	49.4			63.3	5.5					

Uno *et al. Earth, Planets and Space*   *(2021) 73:132*

Page 7 of 17

Table 1 (continued)

Site	Formation	Lithology	N (n)	In situ		Tilt corrected		I corrected	k	α_{95} (°)	Locality		Strike (°)	Dip (°)	IRM$_Z$/IRM$_X$
				D (°)	I (°)	D (°)	I (°)	D (°)	I (°)			Lat (°N)	Long (°E)		
9% unfolded mean								58.3	50.5	82.0	4.8				

ms: mudstone; ss, sandstone; *N(n)*: number of samples used in calculation of the means (number of samples demagnetized); *D* and *I*: declination and inclination, respectively; *k*: the precision parameter; α_{95}: radius of the cone of 95% confidence; Lat: north latitude; Long: east longitude

[a] Not involved in the calculation of the mean direction

[b] Recalculated at the reference point of this study (34.55° N, 133.46° E)

Uno *et al. Earth, Planets and Space*   (2021) 73:132

Page 8 of 17
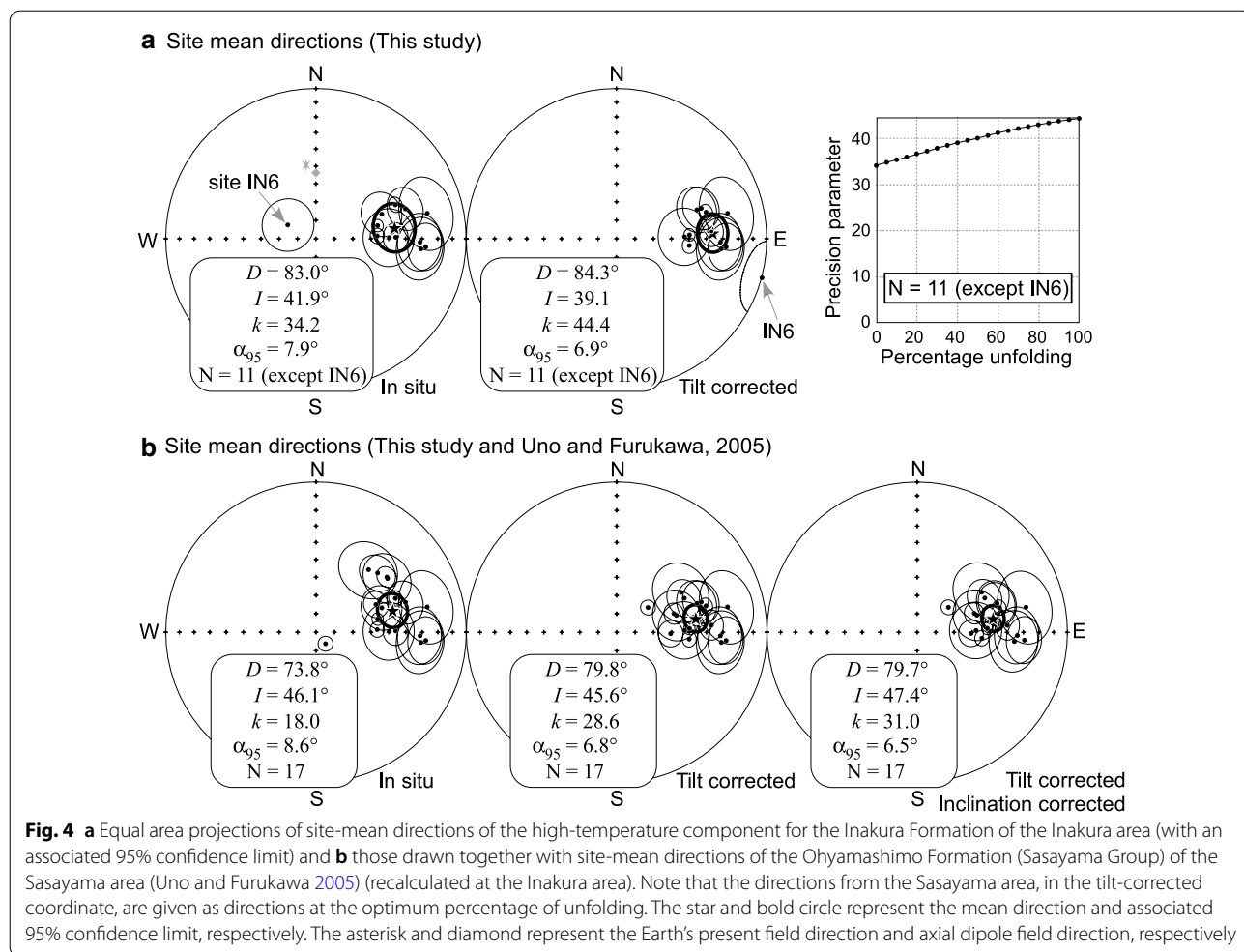
Fig. 4 a Equal area projections of site-mean directions of the high-temperature component for the Inakura Formation of the Inakura area (with an associated 95% confidence limit) and **b** those drawn together with site-mean directions of the Ohyamashimo Formation (Sasayama Group) of the Sasayama area (Uno and Furukawa 2005) (recalculated at the Inakura area). Note that the directions from the Sasayama area, in the tilt-corrected coordinate, are given as directions at the optimum percentage of unfolding. The star and bold circle represent the mean direction and associated 95% confidence limit, respectively. The asterisk and diamond represent the Earth's present field direction and axial dipole field direction, respectively

tilt-corrected $\xi_2 = 3.01$, and a critical value of $\xi = 3.87$ (Fig. 4a), indicating a pre-folding origin. As the tilting of the Inakura Formation occurred prior to 100 Ma, the high-temperature component was interpreted to be primary in nature, corresponding to the Early Cretaceous (110 Ma).

The medium-temperature component was retrieved from 12 sites (IN1–IN3, IN5, IN7–IN14) and showed normal polarity. The mean direction, before tilt correction was $D = 58.2°$ and $I = 50.6°$ with $\alpha_{95} = 4.8°$, and after tilt correction, $D = 59.9°$ and $I = 49.4°$ with $\alpha_{95} = 5.5°$ (Table 1). These directions did not coincide with the Earth's present field direction or the predicted direction from the geocentric axial dipole field. Incremental unfolding was applied to the directions, and the highest value of the precision parameter was observed at 9% unfolding: $D = 58.3°$ and $I = 50.5°$ with $\alpha_{95} = 4.8°$ (Table 1). Apparently, this component has a syn-folding nature, although the direction is almost identical to that before tilt correction. Notably, the 9% unfolded direction (estimated magnetization age of ~100 Ma based on the

folding age) does not coincide with the 100 Ma direction for southwest Japan (Otofuji and Matsuda 1987). Doh et al. (2002) argued that a test result in which optimum grouping is achieved at less than ~30% unfolding does not necessarily represent true syn-folding magnetization. We interpreted the medium-temperature component as a post-folding remanence following complete folding of the strata. The magnetization age was constrained to be between 70 and 20 Ma through comparison with paleomagnetic directions (poles) for southwest Japan.

Rock magnetism

Progressive thermal demagnetization of the three-component IRM of the collected samples showed that remanent magnetization is predominantly retained by hematite, along with a minor contribution from magnetite. The high- (2.5 T) and medium-coercivity (0.4 T) magnetizations were found to be dominant and showed a relatively gradual decay up to 650 °C, after which the remanent magnetization abruptly decayed and was unblocked at temperatures of ~680 °C (Fig. 5). The
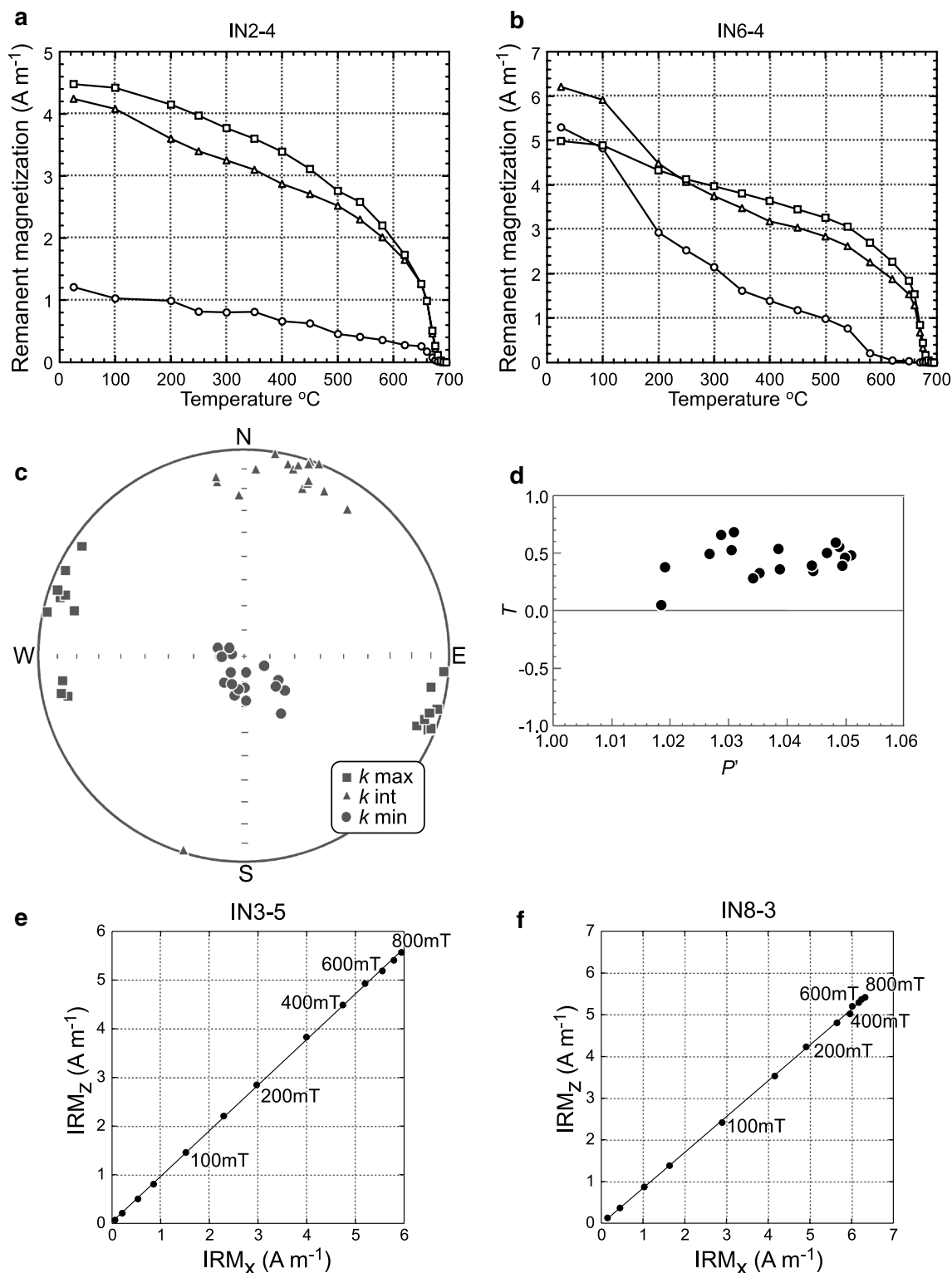
Fig. 5 Rock magnetic results of red mudstone. **a**, **b** Thermal demagnetization of the orthogonal three-component IRM: circles indicate the low-coercivity component (0.12-T) field, triangles indicate the medium-coercivity component (0.4-T) field, and squares indicate the high-coercivity component (2.5-T) field. **c**, **d** Anisotropy of magnetic susceptibility (AMS) results. Orientations of the principal axes of magnetic susceptibility in stratigraphic coordinates (lower hemisphere projection) and plot of shape parameter *T* versus degree of anisotropy *P'* (Jelínek, 1981). **e**, **f** Plot of IRM_Z versus IRM_X showing the gradient of the best-fit correlation line, providing an estimate of the inclination shallowing in sediments

Uno *et al. Earth, Planets and Space* (2021) 73:132

Page 10 of 17

low-coercivity (0.12 T) magnetization was weak, and either no particular mineral phase (Fig. 5a) or minor amounts of magnetite (Fig. 5b) were observed.

The AMS results reveal sedimentary fabrics in stratigraphic coordinates with the k_{min} axis almost perpendicular to the bedding (Fig. 5c, d). Oblate fabrics are predominant, and the average P' value is < 1.04. Our observations indicate that the sampled strata were not significantly deformed by subsequent tectonic activities.

We calculated the IRM_Z/IRM_X ratio for each site and applied it to the tilt-corrected inclination (Fig. 5e, f, Table 1). The results indicated that the inclination flattening for the sites was up to 5.0°. The mean tilt-corrected direction of the Inakura Formation, after inclination correction, was $D = 84.2°$ and $I = 41.9°$ with $\alpha_{95} = 7.1°$ ($N = 11$). This direction can be regarded as the representative direction of the Inakura area in the Early Cretaceous (110 Ma).

Optical observations

To identify the occurrence and textural positions of iron oxides in the sampled rock, microscopic observations were conducted under reflected light. Subangular to subrounded Fe–Ti oxide grains, up to tens of micrometers, were sporadically distributed in the thin sections (Fig. 6), indicating that these grains exist as detrital particles. The grains revealed a distinctive reflection pleochroism, indicating the presence of an ilmenite–hematite solid solution series (Battey 1967). These detrital hematite grains are interpreted as specular hematite. In addition, pigmentary hematite was observed as a reddish matrix surrounding the detrital grains (Fig. 6). Specular hematite typically has higher unblocking temperatures (above 650 °C) and carries primary detrital remanent magnetization (DRM), whereas pigmentary hematite exhibits lower unblocking temperatures and possesses secondary chemical remanent magnetization (CRM) through

pigmentation (Jiang et al. 2015). The observed high-temperature component had unblocking temperatures ranging from 670 to 695 °C and is therefore considered to be carried by specular hematite as DRM.

Discussion

Construction of an APWP for southwest Japan

Through this study, we attempted to obtain a more accurate estimate of the Early Cretaceous (~110 Ma) paleomagnetic pole, representative of southwest Japan. At present, the only available 110 Ma paleomagnetic data are from the Sasayama area (Sy; Fig. 1a). Three studies have presented paleomagnetic poles for this area (Shibuya and Sasajima 1984; Uno and Furukawa 2005; Tsuji and Morinaga 2008). The data from Uno and Furukawa (2005) and Tsuji and Morinaga (2008) are reliable and could be representative of southwest Japan, while those from Shibuya and Sasajima (1984) are not. The poles by Uno and Furukawa (2005) and Tsuji and Morinaga (2008) are statistically similar to each other; however, the poles by Shibuya and Sasajima (1984) are significantly different from the others with high uncertainty (Fig. 1b). Shibuya and Sasajima (1984) considered that the second highest temperature component during thermal demagnetization is the primary component; however, a fold test for this component was not available. In contrast, the reliability of the data of Uno and Furukawa (2005) and Tsuji and Morinaga (2008) was evaluated based on the fold test, and can be incorporated into the coeval paleomagnetic dataset. However, the study by Tsuji and Morinaga (2008) was published as an abstract, and their results were not presented as site-based data but as an overall group-mean direction. Therefore, we incorporated only the data of Uno and Furukawa (2005) into the 110 Ma dataset for southwest Japan. As the sediments of the Sasayama area were deposited in a syn-folding sedimentary basin (Yoshikawa 1993), the best grouping in the observed
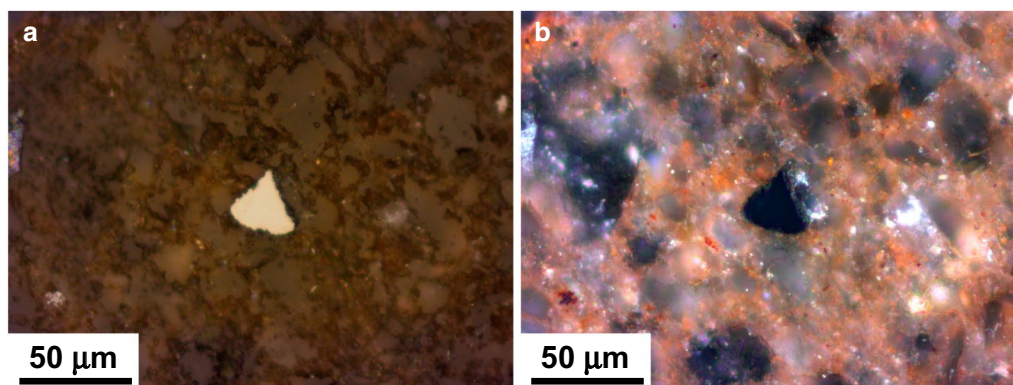

Fig. 6 Photomicrographs of sample IN3-5 in **a** plane and **b** polarized reflected light, showing hematite grain as detrital particles

Uno *et al. Earth, Planets and Space*   (2021) 73:132

Page 11 of 17

directions was attained during the incremental unfolding process (Uno and Furukawa 2005; Tsuji and Morinaga 2008). Therefore, we incorporated the six site-mean directions of the Sasayama area, at the optimum percentage of unfolding, in the tilt-corrected directions of the Inakura area obtained in this study (Fig. 4b). To obtain a new 110 Ma paleomagnetic pole for southwest Japan, the directions of the Sasayama area were recalculated from the reference point of the Inakura area (34.55° N, 133.46° E). The paleomagnetic directions of the Inakura and Sasayama areas were averaged at the reference point to yield a mean direction ($D = 79.7°$, $I = 47.4°$, $\alpha_{95} = 6.5°$, $N = 17$; Fig. 4b), and a paleomagnetic pole at 24.6° N, 203.1° E with $A_{95} = 6.8°$ (Fig. 7a, Table 2). This pole was derived from an area covering a distance of 170 km in southwest Japan.

In addition to the 110 Ma pole, we derived the paleomagnetic pole positions for southwest Japan during the Late Cretaceous in time steps of 10 million years, where 90, 80, and 70 Ma poles were obtained (Table 2). We recalculated the paleomagnetic poles used in Uno et al. (2017), except those derived from data of plutonic rocks (Ito and Tokieda 1978) and those where tilt correction resulted in dispersion in the assessed direction (Fukuma et al. 2003). The paleomagnetic pole of 90 Ma was calculated based on the data from two areas within southwest Japan (Onogawa and San'in areas; O and Si in Fig. 1a), yielding a mean pole located at 29.6° N, 200.3° E with $A_{95} = 8.7°$ and $N = 22$. This pole covers a distance of approximately 250 km in southwest Japan. The 80 Ma pole was calculated using data from the San'in and Ikuno areas (Si and iK; Fig. 1a), and the mean pole was located at 27.0° N, 207.7° E with $A_{95} = 8.9°$ and $N = 13$. This pole covers a distance of approximately 200 km in southwest Japan. The 70 Ma pole was recalculated using data from the Izumi area (iZ in Fig. 1a; Kodama 1990). Kodama (1990) presented magnetostratigraphic data between the Campanian and the Early Maastrichtian of the Late Cretaceous. We extracted the data near the Campanian–Maastrichtian boundary to obtain a recalculated pole located at 27.6° N, 203.9° E with $A_{95} = 12.4°$ and $N = 21$. This pole spans approximately 11 km in stratigraphic thickness. It seems unlikely that the 90–70 Ma poles suffered significant inclination shallowing. The data for the 90 and 80 Ma poles were derived from igneous rocks (welded tuffs), whereas those for the 70 Ma pole were from sedimentary rocks; however, this pole location is similar to the other Cretaceous poles, in terms of predicted inclination in southwest Japan.

For Cenozoic poles of southwest Japan, we referred to the well-established Early Miocene (20 Ma) and Middle Miocene (12 Ma) data. Paleomagnetic poles of 20 and 12 Ma for southwest Japan were compiled using data
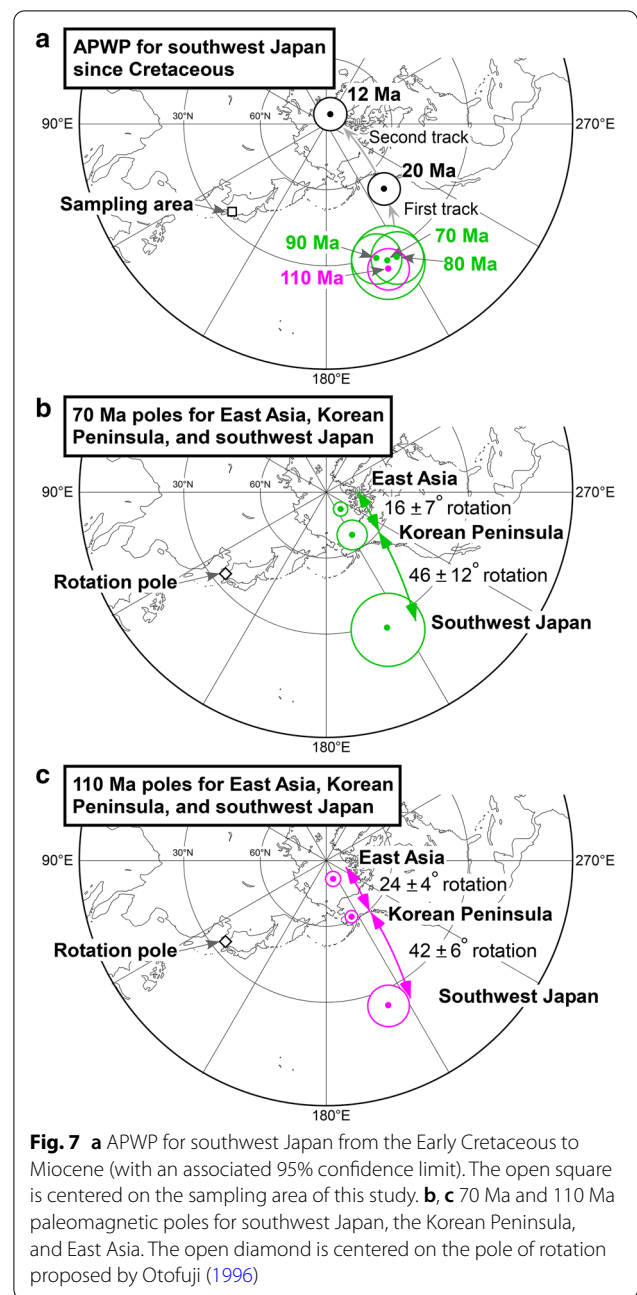
Fig. 7 a APWP for southwest Japan from the Early Cretaceous to Miocene (with an associated 95% confidence limit). The open square is centered on the sampling area of this study. **b, c** 70 Ma and 110 Ma paleomagnetic poles for southwest Japan, the Korean Peninsula, and East Asia. The open diamond is centered on the pole of rotation proposed by Otofuji (1996)

from five and four studies, respectively (Uno et al. 2017) (Table 2). The poles cover distances of more than 250 km in this region. They are located at 51.3° N, 221.3° E with $A_{95} = 6.7°$ (20 Ma) and 85.3° N, 340.4° E with $A_{95} = 7.7°$ (12 Ma; Fig. 7a), respectively.

The APWP for southwest Japan has been renewed since the Cretaceous onward, and is composed of six stages at 110, 90, 80, 70, 20, and 12 Ma (Fig. 7a). This APWP is a revised version from that of Uno et al. (2017), and is also intended to supersede the previous APWP models by Otofuji and Matsuda (1987) and Kodama and Takeda

Uno *et al. Earth, Planets and Space* (2021) 73:132

Page 12 of 17

Table 2 Paleomagnetic poles for southwest Japan, Korean Peninsula, and East Asia

Stage	Age	N	Pole		A₉₅ (°)	References
			Lat (°N)	Long (°E)	A_{95} (°)	
Southwest Japan						
12 Ma	12 ± 1 Ma	4	85.3	340.4	7.7	Uno et al. (2017)
20 Ma	20 ± 4 Ma	5	51.3	221.3	6.7	Uno et al. (2017)
70 Ma	74 ± 2 Ma	(21)	27.6	203.9	12.4	Kodama (1990)[a]
80 Ma	82 ± 2 Ma	(13)	27.0	207.7	8.9	Otofuji and Matsuda (1987), Uno (2002)
90 Ma	89 ± 2 Ma	(22)	29.6	200.3	8.7	Otofuji and Matsuda (1987), Uno et al. (2017)
110 Ma	111 ± 6 Ma	(17)	24.6	203.1	6.8	This study, Uno and Furukawa (2005)
Korean Peninsula						
70 Ma	72 ± 3 Ma	(14)	67.0	210.6	6.7	Kang and Kim (2000)
110 Ma	110 ± 1 Ma	9	61.8	203.8	2.7	Lee et al. (2011)[a]
East Asia						
70 Ma		45	79.7	219.5	3.3	Cogné et al. (2013)
110 Ma		22	80.8	199.5	3.5	Cogné et al. (2013)

N: number of studies (sites) used in calculation of the means; Lat: north latitude; Long: east longitude; A_{95}: radius of the circle of 95% confidence

[a] Mean pole recalculated for this study

(2002), covering the widest chronological range. The proposed APWP does not include Paleogene data by Otofuji and Matsuda (1987), since they were not averaged over a wide area of southwest Japan. Nevertheless, this APWP is important for identifying the paleomagnetism trends of the Asian continent, while trying to build an APWP database for every 10 million years (e.g., Cogné et al. 2013; Van der Voo et al. 2015; Huang et al. 2018a; Ren et al. 2018; Jeong and Yu 2019).

Relative motion of southwest Japan and its vicinity with respect to the interior of Asia

Features of the APWP for southwest Japan

The APWP for southwest Japan has been observed to have experienced a standstill during 110–70 Ma (Fig. 7a). The quiescence in polar motion during this time interval appears to be consistent with the ~130–70 Ma stagnation of pole positions for East Asia as well as Europe (Torsvik et al. 2012; Cogné et al. 2013), referred to as the Cretaceous standstill (Besse and Courtillot 1991; Jeong and Yu 2019). Otofuji and Matsuda (1987) reported that the period of standstill for southwest Japan was rather long and estimated to be between 100 and 20 Ma. The long duration of the standstill is ascribed to the pole position of 20 Ma (37.9° N, 216.9° E with $A_{95} = 10.9°$) from Otofuji and Matsuda (1987), which is located at a lower latitudinal position than the coeval pole (51.3° N, 221.3° E with $A_{95} = 6.7°$), and is close to their Cretaceous poles. As the pole of 20 Ma of Otofuji and Matsuda (1987) is derived from a single area (San'in area; Fig. 1a), we posit that their pole data need to be improved by combining their data with those from other areas of southwest Japan.

The APWP for southwest Japan effectively outlines the rotational history of this region from the Cretaceous. There are three groups and two tracks in the pole position. The first track was observed between 70 and 20 Ma (Fig. 7a). The 70 Ma pole is significantly shifted (by 27.1° ± 14.1°) from the 20 Ma pole. This difference is described as a paleomagnetic rotation of 30.9° ± 11.9°, calculated from the reference point of this study (34.55° N, 133.46° E, at the sampling area), as a poleward displacement (3.1° ± 10.2°) is not significant between these poles from the reference point. The second track in the APWP for southwest Japan was observed between 20 and 12 Ma (Fig. 7a). The 20 Ma pole was found to have shifted by 41.2° ± 10.2° from the 12 Ma pole. The difference in pole position can be explained by a paleomagnetic rotation of 47.3° ± 8.6°. No significant poleward displacement (2.8° ± 6.8°) was observed between the two poles. These observations show that the APWP for southwest Japan records multiphase rotations in the pole position after the Cretaceous.

Here, we propose a post-Cretaceous tectonic scenario that includes two phases of clockwise rotation of southwest Japan: (1) clockwise rotation of ~20° when attached to the Korean Peninsula, due to intra-cratonic rifting during the Paleogene, and (2) clockwise rotation of ~40°–50°, in association with the opening of the Japan Sea during the Neogene. These tectonics resulted in a total rotation of approximately 60–70° for southwest Japan.

First rotation

We observed that the Late Cretaceous paleomagnetic pole for the Korean Peninsula does not coincide with the coeval pole for the interior part of East Asia (hereafter referred to as East Asia) (Fig. 7b). The 70 Ma pole for the Korean Peninsula is located at 67.0° N, 210.6° E with $A_{95}=6.7°$ (Kang and Kim 2000), which is a significantly lower latitude than that for East Asia at 79.7° N, 219.5° E with $A_{95}=3.3°$ (Cogné et al. 2013). This discrepancy would suggest tectonic rotation of the Korean Peninsula relative to East Asia. The amount of rotation may be calculated at a pivot point of rotation (34.0° N, 129.0° E), as proposed by Otofuji (1996), which is located midway between the Korean Peninsula and southwest Japan. A clockwise rotation of $15.5°\pm6.6°$ (with a negligible poleward displacement of $-0.9°\pm5.5°$) of the Korean Peninsula was evaluated to have occurred after 70 Ma.

The clockwise rotation observed from 110 Ma poles between the Korean Peninsula and East Asia is consistent with that observed from 70 Ma poles, corroborating that the tectonic rotation of the Korean Peninsula occurred after 70 Ma (Fig. 7c). We calculated a 110 Ma pole for the Korean Peninsula based on nine poles of this age, which was a recalculation for the compilation of Lee et al. (2011). Thus, we obtained a pole position at 61.8° N, 203.8° E with $A_{95}=2.7°$. This pole showed a clockwise rotation of $23.8°\pm4.0°$ (with a negligible poleward displacement of $0.1°\pm3.2°$) relative to that for East Asia at 80.8° N, 199.5° E with $A_{95}=3.5°$ (Cogné et al. 2013), calculated at the pivot point of Otofuji (1996). The consistent relative rotation between 110 and 70 Ma suggests that the Korean Peninsula was tectonically quiescent in terms of rotation during this interval. This is also consistent with the 110–70 Ma polar standstill for southwest Japan.

The rotation of the Korean Peninsula is likely to have been accompanied by the rotation of southwest Japan. During the Paleogene period, due to the absence of the Japan Sea, southwest Japan was flanked by the Korean Peninsula in the west and formed a single tectonic block (Kojima 1989; Hayashida et al. 1991; Kojima et al. 2000; Otofuji et al. 2003; Itoh et al. 2006). The geographically direct connection between the Korean Peninsula and southwest Japan (i.e., absence of a basin topography of the Japan Sea) was inferred from the supply of sediments from southwest Japan to the Korean Peninsula. Mitsugi et al. (2001) discovered the presence of Permian to Jurassic chert pebbles in the Cretaceous strata in the southeastern part of the Korean Peninsula (Kyongsang Supergroup), where Permian–Jurassic marine chert sequence has not been reported. The pebbles yield radiolarian fauna that are correlated with those reported from a Jurassic accretionary complex in southwest Japan (Mino–Tamba terrane). Furthermore, the pebble-bearing strata showed signatures of a southwestward paleocurrent, explaining the sediment transportation from southwest Japan to the southeastern part of the Korean Peninsula (Chough and Sohn 2010).

We suggest that the clockwise rotation observed in the Korean Peninsula, which corresponds to the first clockwise rotation for southwest Japan, occurred in association with intra-cratonic rifting that resulted in the formation of extensional basins, such as the Bohai Bay Basin, Yilan–Yitong Graben, and Songliao Basin (Fig. 1a). Graben structures were identified in the Bohai Bay Basin. Huang et al. (2015, 2018b) conducted a seismic reflection survey and showed that the oldest basin fill sediments are ~65 Ma in age. The boundary faults forming the graben are terminated by the overlying sediments of ~40 Ma, suggesting extensional deformation during 65–40 Ma. Li et al. (2017) analyzed the thermal history of the Bohai Bay Basin by estimating the surface and mantle heat flow through geological time. An increase in the ratio of mantle heat flow to surface heat flow occurred between 50 and 45 Ma, indicating that this basin underwent rifting and crustal thinning during the Paleogene. Paleogene extensional structures were also identified in the Yilan–Yitong Graben, where the sediment thickness is more than 4000 m, at the maximum (Gu et al. 2017). Yin (2010) and Song et al. (2018) suggested that the peak of basaltic magmatism at ~60–40 Ma, in the Songliao Basin, was a result of a large-scale crustal extension in this region. These Paleogene rifting activities played an important role in the observed tectonic rotation.

The distribution of these extensional basins suggests that a wider area have undergone a tectonic rotation, and the influence of this rotation extended till the vicinity of the Tan-Lu Fault. Paleomagnetic data corresponding to the Paleogene clockwise rotation are also available from Benxi, northeast China (Bx; Fig. 1a). Uchimura et al. (1996) and Lin et al. (2003) conducted paleomagnetic studies of Late Cretaceous deposits, and observed a clockwise rotation of 18–23° with respect to East Asia. These authors revealed that the clockwise deflected paleomagnetic directions were exclusively observed to the east of the Tan-Lu Fault and its northern extension (Yilan–Yitong Fault; Fig. 1a). This implies that the single rotational tectonic unit incorporated northeast China, the Korean Peninsula, and southwest Japan. This was referred to as the East Tan-Lu Block by Itoh et al. (2006) and the East Liaoning-Korea Block by Lin et al. (2003). As southwest Japan was located at an integral part of the East Tan-Lu Block throughout the Paleogene, the clockwise rotation during this time, observed for southwest Japan, needs to be discussed in the context of the tectonic rotation of this particular block (Otofuji et al. 2003, 2006; Zhou et al. 2019).

We integrated the relevant findings to define the spatial extent of the phenomenon. It is believed that the rotated region is the area east of the Tan-Lu Fault, as proposed by Ma et al. (1993), with easterly deflected declination observed in North and South Korea and the Jiaodong Peninsula. The Cretaceous and younger polar motions in this region were systematically shifted from those of the North China Block. Uchimura et al. (1996) attributed the driving force of the tectonic rotation to post-Cretaceous large-scale sinistral faulting, up to ~800 km, along the Tan-Lu Fault. Although it was an active sinistral fault during the period when the first clockwise rotation is estimated to have occurred (Wang et al. 2019), geological evidence does not suggest such large post-Cretaceous sinistral offsets. Lin et al. (2003) proposed a clockwise tectonic rotation (i.e., first-phase rotation), primarily based on paleomagnetic data from the Benxi area and the Korean Peninsula (Fig. 1a). The region of inferred clockwise rotation is not limited to Benxi and the Korean Peninsula, but extends to Far East Russia (Sikhote Alin; Fig. 1a). This tectonic interpretation by Lin et al. (2003) opposes that of Otofuji et al. (2003) in terms of the sense of rotation of Sikhote Alin. Lin et al. (2003) concluded their study without evaluating the paleomagnetic data from Sikhote Alin, whereas Otofuji et al. (2003) obtained Late Cretaceous (~74–66 Ma) paleomagnetic data from the area, showing westerly deflection and interpreted that the region suffered counter-clockwise tectonic rotation. Wang et al. (2011) delineated the northern limits of the clockwise rotational motion, providing Paleogene paleomagnetic data from Ning'an, northeast China (Na; Fig. 1a), which exhibits a clockwise rotation (~26°) relative to the coeval data for the continental interior. This area is also interpreted as being located to the east of the Tan-Lu fault system. Counter-clockwise rotation was dominant to the north of that area. Huang et al. (2007) analyzed available Cretaceous paleomagnetic data for the area east of the Tan-Lu Fault, and concluded that the first clockwise rotation affected the Liaodong Peninsula to the southwest of Benxi but did not affect the Jiaodong Peninsula (Fig. 1a). The authors postulated that the northern extent of the clockwise rotational motion corresponds to the Mudanjiang Fault (Fig. 1a). These studies verified the spatial effects of the first clockwise rotation by developing a geodynamically coherent framework for the East Tan-Lu Block. The first clockwise rotation for southwest Japan is inferred to have occurred as part of the East Tan-Lu Block, and associated with Paleogene rifting while the area was attached to the Korean Peninsula.

Second rotation

Following the Paleogene rifting, southwest Japan rifted from the Korean Peninsula in the Neogene. As a consequence of this rifting, southwest Japan underwent further clockwise rotation (Otofuji et al. 1991; Hoshi et al. 2015; Ishikawa et al. 2017). The degree of rotation for southwest Japan may be calculated as the rotation angle with respect to both East Asia and the Korean Peninsula, since the corresponding paleomagnetic poles were statistically similar during the Neogene. For example, the Miocene pole for East Asia [84.7° N, 255.9° E, $A_{95} = 3.1°$, 20 Ma, Cogné et al. (2013)] and that for the Korean Peninsula [83.3° N, 251.8° E, $A_{95} = 5.4°$, <17 Ma, Son et al. (2013)] are in almost the same position. Based on this idea, Hoshi et al. (2019) estimated the degree of rotation for southwest Japan to be 35–42° by comparing it with that of East Asia. When we calculated the degree of rotation using the 20 Ma pole of our study with respect to the coeval poles for East Asia and the Korean Peninsula, at a rotation pivot of 34.0° N, 129.0° E of Otofuji (1996), the amount of rotation was evaluated to be $38.5° \pm 6.0°$ and $36.9° \pm 7.1°$, respectively.

The rifting resulted in the formation of the Japan Sea. The timing of the formation of the basaltic oceanic crust of the Japan Sea was evaluated to be 21.2–14.9 Ma, based on drilling results and geochronological data (Pisciotto and Ingle Jr. 1990; Kaneoka et al. 1992; Nohda 2009). This timing is similar to that of the paleomagnetic rotation of ~17.5–14.2 Ma (Baba et al. 2007; Hoshi et al. 2015), but the onset of paleomagnetic rotation is slightly younger than that of the obtained age of the Japan Sea basalts. Hayashida et al. (1991) analyzed the paleomagnetic data and found that the early stages of rifting in southwest Japan occurred in the form of southeastward translation from the margin, which was followed by rotational (i.e., fan-shaped) rifting in the later stages.

Periodic extension models

Southwest Japan twice experienced clockwise tectonic rotation, in response to the rifting activities in the margin of the Asian continent during the Cenozoic. The two rifting events can be explained using a periodic extension model. Based on the two-dimensional mantle convection model (Lowman and Jarvis 1996), Otofuji et al. (2003, 2006) argued that periodic eastward flow of the asthenosphere twice caused rifting of the Asian continental margin. Lowman and Jarvis (1996) described that asthenospheric upwelling beneath the continental margin occurs intermittently following the growth of a megacontinent by continental collision. This upwelling induces lateral mantle flow beneath a continent and drives the oceanward rifting of continental fragments. During the Cenozoic, the eastern margin of the Asian continent most likely encountered intermittent tectonics, since the complete suturing of Asia and Siberia–Europe had occurred to form the Eurasian mega-continent during

the Cretaceous (Cogné et al. 2005; Metelkin et al. 2010; Van der Voo et al. 2015). The suture zone corresponding to the collision is the Mongol–Okhotsk suture, where the size of each colliding continental landmass is of the order of thousands of kilometers. This corresponds to the size of the collisional continents assumed by Lowman and Jarvis (1996). The site of the present Japanese islands was situated at the eastern margin of the Asian continent during the Mesozoic to Early Cenozoic and could be an example of possible intermittent tectonics.

Deep mantle processes and the associated dynamics of the Eurasian–Paleo-Pacific subduction system provide an alternative source of the multiphase extension. Based on the analysis of tectono-magmatic activities in the eastern North China Block, Liu et al. (2021) argued that eastward flow of the deep mantle at 160 Ma induced eastward migration of the shallow mantle convection systems. This continuously drove the retreating subduction of the Paleo-Pacific plate with the eastward migration of the Paleo-Pacific–Farallon mid-oceanic ridge, leading to multiple phases of extensional tectonics at the Eurasian continental margin. It is possible that southwest Japan, as part of the Eurasian continental margin, suffered two of these periodic extensions during the post-Cretaceous period.

Concluding remarks

We constructed the APWP for the inner arc of the southwestern Japanese islands (southwest Japan) from the Early Cretaceous. The pole position was observed to be stationary between 110 and 70 Ma, suggesting that southwest Japan behaved as a stable part of the Asian continental margin during the Cretaceous. The Cenozoic APWP for southwest Japan includes two large tracks. We interpret these tracks as clockwise tectonic rotations of southwest Japan that occurred twice in the Cenozoic. The earlier rotation occurred during the Paleogene, when southwest Japan was attached to the Korean Peninsula, as part of the East Tan-Lu Block. During the Neogene, the later rotation occurred, and southwest Japan detached from the East Tan-Lu Block to form the Japan Sea. We suspect that periodic eastward flow of the asthenosphere caused rifting of the Asian continental margin twice, likely due to a large-scale continental collision that formed the Eurasian continent.

Abbreviations

APWP: Apparent polar wander path; IGRF: International Geomagnetic Reference Field; NRM: Natural remanent magnetization; MAD: Maximum angular deviation; IRM: Isothermal remanent magnetization; AMS: Anisotropy of magnetic susceptibility; DRM: Detrital remanent magnetization; CRM: Chemical remanent magnetization.

Author details

[1]Department of Earth Sciences, Okayama University, 3-1-1 Tsushimanaka, Kita-ku, Okayama 700-8530, Japan. [2]Faculty of Business Administration, Aichi University, 4-60-6 Hiraike-cho, Nakamura-ku, Nagoya 453-8777, Japan.

References

Baba AK, Matsuda T, Itaya T, Wada Y, Hori N, Yokoyama M, Eto N, Kamei R, Zaman H, Kidane T, Otofuji Y (2007) New age constraints on counter-clockwise rotation of NE Japan. Geophys J Int 171:1325–1341

Battey MH (1967) The identification of the opaque oxide minerals by optical and X-ray methods. In: Collinson DW, Creer KM, Runcorn SK (eds) Methods in paleomagnetism. Elsevier, Amsterdam, pp 254–286

Besse J, Courtillot V (1991) Revised and synthetic apparent polar wander paths of the African, Eurasian, North American and Indian Plates, and true polar wander since 200 Ma. J Geophys Res 96:4029–4050

Chough SK, Sohn YK (2010) Tectonic and sedimentary evolution of a Cretaceous continental arc–backarc system in the Korean peninsula: new view. Earth Sci Rev 101:225–249

Cogné JP (2003) PaleoMac: a Macintosh[TM] application for treating paleomagnetic data and making plate reconstructions. Geochem Geophys Geosyst 4:1007. https://doi.org/10.1029/2001GC000227

Cogné JP, Kravchinsky VA, Halim N, Hankard F (2005) Late Jurassic-Early Cretaceous closure of the Mongol-Okhotsk Ocean demonstrated by new Mesozoic palaeomagnetic results from the Trans-Baikal area (SE Siberia). Geophys J Int 163:813–832

Cogné JP, Besse J, Chen Y, Hankard F (2013) A new Late cretaceous to present APWP for Asia and its implications for paleomagnetic shallow inclinations in Central Asia and Cenozoic Eurasian plate deformation. Geophys J Int 192:1000–1024

Doh SJ, Kim W, Suk D, Park YH, Cheong D (2002) Palaeomagnetic and rock-magnetic studies of Cretaceous rocks in the Gongju Basin, Korea: implications for clockwise rotation. Geophys J Int 150:737–752

Enkin RJ, Yang Z, Chen Y, Courtillot V (1992) Palaeomagnetic constraints on the geodynamic history of the major blocks of China from the Permian to the present. J Geophys Res 97:13953–13989

Uno *et al. Earth, Planets and Space*   (2021) 73:132

Page 16 of 17

Fukuma K, Tsurudome H, Torii M (2003) A Late Cretaceous paleomagnetic pole from Koto rhyolite, southwest Japan: implications for eastern margin deformation of Asia. J Geophys Res 108:2544. https://doi.org/10.1029/2001JB000425

Gilder S, Courtillot V (1997) Timing of the North-South China collision from new middle to late Mesozoic paleomagnetic data from the North China Block. J Geophys Res 102:17713–17727

Gu C, Zhu G, Zhang S, Liu C, Li Y, Lin S, Wang W (2017) Cenozoic evolution of the Yilan-Yitong Graben in NE China: an example of graben formation controlled by pre-existing structures. J Asian Earth Sci 146:168–184

Hatakeyama T (2018) Online plotting applications for paleomagnetic and rock magnetic data. Earth Planets Space 70:139

Hayashida A, Fukui T, Torii M (1991) Paleomagnetism of the Early Miocene Kani Group in Southwest Japan and its implication for the opening of the Japan Sea. Geophys Res Lett 18:1095–1098

Hodych JP, Buchan KL (1994) Early Silurian palaeolatitude of the Springdale Group redbeds of central Newfoundland: a palaeomagnetic determination with a remanence anisotropy test for inclination error. Geophys J Int 117:640–652

Hoshi H (2018) Miocene clockwise rotation of Southwest Japan. J Geol Soc Jpn 124:675–691

Hoshi H, Kato D, Ando Y, Nakashima K (2015) Timing of clockwise rotation of Southwest Japan: constraints from new middle Miocene paleomagnetic results. Earth Planets Space 67:92–104

Hoshi H, Iwano H, Danhara T, Oshida H, Hayashi H, Kurihara Y, Yanagisawa Y (2019) Age of the N7/N8 (M4/M5) planktonic foraminifera zone boundary: constraints from the zircon geochronology and magnetostratigraphy of early Miocene sediments in Ichishi, Japan. Chem Geol 530:119333

Huang B, Piper JDA, Zhang C, Li Z, Zhu R (2007) Paleomagnetism of Cretaceous rocks in the Jiaodong Peninsula, eastern China: insight into block rotations and neotectonic deformation in eastern Asia. J Geophys Res 112:B03106. https://doi.org/10.1029/2006JB004462

Huang L, Liu CY, Kusky TM (2015) Cenozoic evolution of the Tan–Lu Fault Zone (East China)—constraints from seismic data. Gondwana Res 28:1079–1095

Huang B, Yan Y, Piper JDA, Zhang D, Yi Z, Yu S, Zhou T (2018a) Paleomagnetic constraints on the paleogeography of the East Asian blocks during Late Paleozoic and Early Mesozoic times. Earth Sci Rev 186:8–36

Huang L, Liu CY, Xu CG, Wu K, Wang GY, Jia N (2018b) New insights into the distribution and evolution of the Cenozoic Tan-Lu Fault Zone in the Liaohe sub-basin of the Bohai Bay Basin, eastern China. Tectonophysics 722:373–382

Imamura S, Kusumi H (1951) On the Inkstone Group of Inakura-mura district, Oda-gun, Okayama Prefecture, Japan. Geol Rep Hiroshima Univ 1:1–14

Imaoka T, Nakajima T, Itaya T (1993) K-Ar ages of hornblendes in andesite and dacite from the Cretaceous Kanmon Group, Southwest Japan. J Miner Petrol Econ Geol 88:265–271

Ishida K, Kozai T, Park SO, Mitsugi T (2003) Gravel bearing radiolaria as tracers for erosional events: a review of the status of recent research in SW Japan and Korea. J Asian Earth Sci 21:909–920

Ishikawa N (1997) Differential rotations of north Kyushu Islands related to middle Miocene clockwise rotation of SW Japan. J Geophys Res 102:17729–17745

Ishikawa N, Suzuki T, Ishida S (2017) Paleomagnetic studies on Miocene sequences of Hokutan and Tottori Groups in Southwest Japan: implications for middle Miocene rotational movement of Southwest Japan block associated with the Japan Sea opening. In: Itoh Y (ed) Evolutionary models of convergent margins—origin of their diversity. Rijeka, INTECH Open Access Book. https://doi.org/10.5772/67960

Isozaki Y (2019) A visage of early Paleozoic Japan: geotectonic and paleobiogeographical significance of Greater South China. Island Arc. https://doi.org/10.1111/iar.12296

Isozaki Y, Aoki K, Nakama T, Yanai S (2010) New insight into a subduction-related orogen: a reappraisal of the geotectonic framework and evolution of the Japanese Islands. Gondwana Res 18:82–105

Ito H, Tokieda K (1978) Paleomagnetism of the Ibaragi granitic complex, vol 12. Memoirs of the Faculty of Science, Shimane University, Matsue, pp 33–43

Itoh Y, Uno K, Arato H (2006) Seismic evidence of divergent rifting and subsequent deformation in the southern Japan Sea, and a Cenozoic tectonic synthesis of the eastern Eurasian margin. J Asian Earth Sci 27:933–942

Jelínek V (1981) Characterization of the magnetic fabric of rocks. Tectonophysics 79:63–67

Jeong D, Yu Y (2019) Apparent polar wander path for East Asia and implications for paleomagnetic low inclination in sedimentary rocks. Phys Earth Planet Int 289:63–72

Jiang Z, Liu Q, Dekkers MJ, Tauxe L, Qin H, Barrón V, Torrent J (2015) Acquisition of chemical remanent magnetization during experimental ferrihydrite–hematite conversion in Earth-like magnetic field—implications for paleomagnetic studies of red beds. Earth Planet Sci Lett 428:1–10

Jolivet L, Tamaki K, Fournier M (1994) Japan Sea, opening history and mechanism: a synthesis. J Geophys Res 99:22237–22259

Kaneoka I, Takigami Y, Takaoka N, Yamashita S, Tamaki K (1992) ^{40}Ar–^{39}Ar analysis of volcanic rocks recovered from the Japan Sea floor: constraints on the age of formation of the Japan Sea. Proc Ocean Drill Progr Sci Results 127/128:819–836

Kang HC, Kim IS (2000) Palaeomagnetism of the Cretaceous Yuchon Group in Kosong area, southern Kyongsang basin. J Korean Earth Sci Soc 21:663–674

Kang HC, Paik IS (2013) Review on the geological ages of the formations in the Gyeongsang Basin, Korea. J Geol Soc Korea 49:17–29

Kimura K (1996) Cretaceous chronostratigraphy of the Kanmon region, Japan and the Kyongsang Basin, Korea. In: 103rd annual meeting of the geological society of japan abstract, pp 80

Kirschvink JL (1980) The least-square line and plane and the analysis of palaeomagnetic data. Geophys J Roy Astron Soc 62:699–718

Kobayashi T (1990) Cretaceous Nippon Island. Fossils 48:35–37

Kodama K (1990) Magtetostratigraphy of the Izumi group along the median tectonic line in Shikoku and Awaji Islands, Southwest Japan. J Geol Soc Jpn 96:265–278

Kodama K, Takeda T (2002) Paleomagnetism of mid-Cretaceous red beds in west-central Kyushu Island, southwest Japan: paleoposition of Cretaceous sedimentary basins along the eastern margin of Asia. Earth Planet Sci Lett 201:233–246

Kojima S (1989) Mesozoic terrane accretion in Northeast China, Sikhote-Alin and Japan regions. Palaeogeogr Palaeoclimatol Palaeoecol 69:213–232

Kojima S, Igor VK, Kametaka M, Ando A (2000) A correlation of accretionary complexes of southern Sikhote-Alin of Russia and the Inner Zone of Southwest Japan. Geosci J 4:175–185

Lee YI (2008) Paleogeographic reconstructions of the East Asia continental margin during the middle to late Mesozoic. Island Arc 17:458–470

Lee YS, Han HC, Hwang JH, Kee WS, Kim BC (2011) Evidence for significant clockwise rotations of the Korean Peninsula during Cretaceous. Gondwana Res 20:904–918

Li Z, Zuo Y, Qiu N, Gao J (2017) Meso-Cenozoic lithospheric thermal structure in the Bohai Bay Basin, eastern North China Craton. Geosci Front 8:977–987

Lin W, Chen Y, Faure M, Wang Q (2003) Tectonic implications of new Late Cretaceous paleomagnetic constraints from Eastern Liaoning Peninsula, NE China. J Geophys Res. https://doi.org/10.1029/2002JB002169

Liu J, Ni J, Chen X, Craddock JP, Zheng Y, Ji L, Hou C (2021) Early Cretaceous tectonics across the North Pacific: new insights from multiphase tectonic extension in Eastern Eurasia. Earth-Sci Rev 217:103552

Lowman JP, Jarvis GT (1996) Continental collisions in wide aspect ratio and high Rayleigh number two-dimensional mantle convection models. J Geophys Res 101:25485–25497

Lowrie W (1990) Identification of ferromagnetic minerals in a rock by coercivity and unblocking temperature properties. Geophys Res Lett 17:159–162

Ma X, Yang Z, Xing L (1993) The Lower Cretaceous reference pole for North China, and its tectonic implications. Geophys J Int 115:323–331

Maruyama S, Isozaki Y, Kimura G, Terabayashi M (1997) Paleogeographic maps of the Japanese Islands: plate tectonic synthesis from 750 Ma to the present. Island Arc 6:121–142

Matsubara M, Sato H, Ishiyama T, Horne AV (2017) Configuration of the Moho discontinuity beneath the Japanese Islands derived from three-dimensional seismic tomography. Tectonophysics 710–711:97–107

Matsuura H, Kurimoto C, Yoshida F, Saito Y, Makimoto H, Toshimitsu S, Iwaya T, Komazawa M, Hiroshima T (2002) Geological map of Japan 1:200,000, Okayama and Marugame. Geological Survey of Japan, pp 8

McFadden PL (1990) A new fold test for palaeomagnetic studies. Geophys J Int 103:163–169

Uno *et al. Earth, Planets and Space* (2021) 73:132

Page 17 of 17

Metelkin DV, Vernikovsky VA, Kazansky AYu, Wingate MTD (2010) Late Mesozoic tectonics of Central Asia based on paleomagnetic evidence. Gondwana Res 18:400–419

Mitsugi T, Ishida K, Woo BG, Chang KH, Park SO, Hirano H (2001) Radiolarian-bearing conglomerate from the Hayang Group, Kyongsang Supergroup, southeastern Korea. J Asian Earth Sci 19:751–763

Miyazaki K, Matsuura H, Ikeda T (2016) Crustal-scale pattern of rising buoyancy of viscous fluids and mid Cretaceous geology related to high-temperature metamorphic belt in northern Kyushu, Japan. In: Japan Geoscience Union Meeting 2016 Abstract, SMP43–05

Murakami N (1985) Late Mesozoic to Paleogene igneous activity in West Chu-goku, Southwest Japan. J Geol Soc Jpn 91:723–742

Nohda S (2009) Formation of the Japan Sea basin: Reassessment from Ar–Ar ages and Nd–Sr isotopic data of basement basalts of the Japan Sea and adjacent regions. J Asian Earth Sci 34:599–609

Otofuji Y (1996) Large tectonic movement of the Japan Arc in late Cenozoic times inferred from paleomagnetism: review and synthesis. Island Arc 5:229–249

Otofuji Y, Matsuda T (1987) Amount of clockwise rotation of Southwest Japan—fan shape opening of the southwestern part of the Japan Sea. Earth Planet Sci Lett 85:289–301

Otofuji Y, Matsuda T, Nohda S (1985) Opening mode of the Japan Sea inferred from the palaeomagnetism of the Japan Arc. Nature 317:603–604

Otofuji Y, Itaya T, Matsuda T (1991) Rapid rotation of southwest Japan—palaeo-magnetism and K-Ar ages of Miocene volcanic rocks of southwest Japan. Geophys J Int 105:397–405

Otofuji Y, Matsuda T, Enami R, Uno K, Nishihama K, Halim N, Su L, Zaman H, Kulin-ich RG, Zimin PS, Matunin AP, Sakhno VG (2003) Late Cretaceous palaeo-magnetic results from Sikhote Alin, far eastern Russia: tectonic implications for the eastern margin of the Mongolia Block. Geophys J Int 152:202–214

Otofuji Y, Miura D, Takaba K, Takemoto K, Narumoto K, Zaman H, Inokuchi H, Kulinich RG, Zimin PS, Sakhno VG (2006) Counter-clockwise rotation of the eastern part of the Mongolia block: early Cretaceous palaeomagnetic results from Bikin, Far Eastern Russia. Geophys J Int 164:15–24

Pisciotto K, Ingle J Jr (1990) Evolution of the Japan Sea. Nature 346:18–20

Racey A (2009) Mesozoic red bed sequences from SE Asia and the significance of the Khorat Group of NE Thailand. Geol Soc Lond Special Publ 315:41–67

Ren Q, Zhang S, Wu H, Liang Z, Miao X, Zhao H, Li H, Yang T, Pei J, Davis GA (2016) Further paleomagnetic results from the ~ 155 Ma Tiaojishan Formation, Yanshan Belt, North China, and their implications for the tectonic evolution of the Mongol-Okhotsk suture. Gondwana Res 35:180–191

Ren Q, Zhang S, Wu Y, Yang T, Gao Y, Turbold S, Zhao H, Wu H, Li H, Fu H, Xu B, Zhang J, Tomurtogoo O (2018) New Late Jurassic to Early Cretaceous paleomagnetic results from North China and Southern Mongolia and their implications for the evolution of the Mongol-Okhotsk Suture. J Geophys Res 123:10370–10398. https://doi.org/10.1029/2018JB016703

Shibuya H, Sasajima S (1984) Fission track ages and paleomagnetism of acidic tuff of the Sasayama Group. In: 75th meeting of the society of terrestrial magnetism and electricity of Japan Abstract, p 190

Son M, Song CW, Kim MC, Cheon Y, Jung S, Cho H, Kim HG, Kim JS, Sohn YK (2013) Crustal deformation, basin development, and tectonic implication in the Southeastern Korean Peninsula. J Geol Soc Korea 49:93–118

Sonehara T, Yagi K, Takeshita H, Aoki K, Aoki S, Otofuji Y, Itaya T (2020) Kibi Plateau: a stable-coherent tectonic unit in the active Japanese Islands. Sci Rep 10:3786. https://doi.org/10.1038/s41598-020-60448-x

Song Y, Stepashko A, Liu K, He Q, Shen C, Shi B, Ren J (2018) Post-rift tectonic history of the Songliao Basin, NE China: cooling events and post-rift uncon-formities driven by orogenic pulses from plate boundaries. J Geophys Res 123:2363–2395

Suzuki S, Asiedu DK, Fujiwara T (2001) Lower Cretaceous fluvial deposits, Hayama Formation, Nariwa area, Okayama Prefecture, southwest Japan. J Geol Soc Jpn 107:541–556

Tachibana T, Suzuki S (2010) Stratigraphy and sedimentary environment of the lower Cretaceous Inakura Formation in the southwestern part of Okayama Prefecture. In: 117th annual meeting of the geological society of Japan Abstract, p 70

Taira A (2001) Tectonic evolution of the Japanese island arc system. Annu Rev Earth Planet Sci 29:109–134

Thébault E, Finlay CC, Beggan CD, Alken P, Aubert J, Barrois O, Bertrand F, Bondar T, Boness A, Brocco L, Canet E, Chambodut A, Chulliat A, Coïsson P, Civet F,

Du A, Fournier A, Fratter I, Gillet N, Hamilton B, Hamoudi M, Hulot G, Jager T, Korte M, Kuang W, Lalanne X, Langlais B, Léger JM, Lesur V, Lowes FJ, Mac-millan S, Mandea M, Manoj C, Maus S, Olsen N, Petrov V, Ridley V, Rother M, Sabaka TJ, Saturnino D, Schachtschneider R, Sirol O, Tangborn A, Thomson A, Tøffner-Clausen L, Vigneron P, Wardinski I, Zvereva T (2015) International geomagnetic reference field: the 12th generation. Earth Planets Space 67:79

Torsvik TH, Van der Voo R, Preeden U, Mac Niocaill C, Steinberger B, Doubrovine PV, van Hinsbergen DJJ, Domeier M, Gaina C, Tohver E, Meert JG, McCaus-land PJA, Cocks LRM (2012) Phanerozoic polar wander, palaeogeography and dynamics. Earth Sci Rev 114:325–368

Tsuji S, Morinaga H (2008) Cretaceous paleo-position of Southwest Japan: paleo-magnetism of the red sandstones from the Cretaceous Sasayama Group. In: Japan Geoscience Union Meeting 2008 Abstract, E111-P008

Uchimura H, Kono M, Tsunakawa H, Kimura G, Wei Q, Hao T, Liu H (1996) Paleo-magnetism of late Mesozoic rocks from northeastern China: the role of the Tan-Lu fault in the North China Block. Tectonophysics 262:301–319

Uno K (2002) Late Cretaceous palaeomagnetic results from Southwest Japan: new insights for early Cenozoic clockwise rotation. Geophys J Int 149:617–624

Uno K, Furukawa K (2005) Timing of remanent magnetization acquisition in red beds: a case study from a syn-folding sedimentary basin. Tectonophysics 406:67–80

Uno K, Furukawa K, Hatanaka Y (2017) An analysis of apparent polar wander path for southwest Japan suggests no relative movement with respect to Eurasia during the Cretaceous. Phys Earth Planet Int 267:19–30

Van der Voo R, van Hinsbergen DJJ, Domeier M, Spakman W, Torsvik TH (2015) Latest Jurassic–earliest Cretaceous closure of the Mongol-Okhotsk Ocean: a paleomagnetic and seismological-tomographic analysis. In: Anderson TH, Didenko AN, Johnson CL, Khanchuk AI, MacDonald JH (eds), Late Jurassic Margin of Laurasia—a record of faulting accommodating plate rotation. Geological Society of America Special Paper 513, pp 589–606

Wang HL, Huang BC, Qiao QQ, Chen JS (2011) Paleomagnetic study on Creta-ceous and Paleogene rocks from eastern Heilongjiang, NE China and its tectonic implications. Chin J Geophys 54:793–806

Wang G, Li S, Wu Z, Suo Y, Guo L, Wang P (2019) Early Paleogene strike-slip transi-tion of the Tan-Lu Fault Zone across the southeast Bohai Bay Basin: con-straints from fault characteristics in its adjacent basins. Geol J 54:835–849

Wu L, Kravchinsky VA, Potter DK (2017) Apparent polar wander paths of the major Chinese blocks since the Late Paleozoic: toward restoring the amalgamation history of east Eurasia. Earth Sci Rev 171:492–519

Xu X, Harbert W, Dril S, Kravchinksy V (1997) New paleomagnetic data from the Mongol-Okhotsk collision zone, Chita region, south-central Russia: implications for Paleozoic paleogeography of the Mongol-Okhotsk ocean. Tectonophysics 269:113–1291

Yan L, Peng H, Zhang S, Zhang R, Kašanin-Grubin M, Lin K, Tu X (2019) The spatial patterns of red beds and Danxia landforms: implication for the formation factors–China. Sci Rep 9:1961

Yang Z, Besse J (2001) New Mesozoic apparent polar wander path for south China: tectonic consequences. J Geophys Res 106:8493–8520

Yin A (2010) Cenozoic tectonic evolution of Asia: a preliminary synthesis. Tectono-physics 488:293–325

Yoshikawa T (1993) Stratigraphy and structure of the Lower Cretaceous Sasayama Group in the Sasayama area, Hyogo Prefecture, Southwest Japan. J Geol Soc Jpn 99:29–38

Zhou Z, Li S, Guo L, Li X, Jiang Z, Liu Y, Li Y, Wang G, Lan H, Guo R, Wang Y, Somer-ville I (2019) Palaeomagnetic assessment of tectonic rotation in Northeast Asia: implications for the coupling of intracontinental deformation and mantle convection. Int Geol Rev. https://doi.org/10.1080/00206814.2019.1689532

Zijderveld JDA (1967) A.C. demagnetization of rocks: analysis of results. In: Collin-son DW, Creer KM, Runcorn SK (eds) Methods in paleomagnetism. Elsevier, Amsterdam, pp 254–286

Publisher's Note